Chemical Engineering Journal 148 (2009) 290–295

Contents lists available at ScienceDirect

Chemical Engineering Journal

journal homepage: www.elsevier.com/locate/cej

Formation mechanism and structure of dynamic membrane in the dynamic membrane bioreactor

Hongbo Liu, Changzhu Yang*, Wenhong Pu*, Jingdong Zhang

College of Environmental Science and Engineering, Huazhong University of Science and Technology, Wuhan 430074, PR China

ARTICLE INFO

Article history:
Received 25 October 2007
Received in revised form 15 July 2008
Accepted 26 August 2008

Keywords:
Dynamic membrane bioreactor
Membrane flux
Membrane resistance
Compressibility
Voidage

ABSTRACT

A dynamic membrane bioreactor (DMBR) was developed by substituting dynamic membrane (DM) for the separation membrane in the submerge membrane bioreactor. The formation mechanism and structure of dynamic membrane were investigated. Firstly, based on the flux behaviors of dynamic membrane under constant filtration pressure, the formation mechanism of dynamic membrane was assumed in a creative way by dividing the formation process of dynamic membrane into four stages, which was then proved by four classic filtration laws. Furthermore, by the proposed formation mechanism, dynamic membrane from inner to outer was divided into three layers, namely substrate layer, separation layer and fouling layer. Moreover, by combining the theory of hydrokinetic boundary layer with the formation mechanism of dynamic membrane, the methods for calculating the optimum cross-flow velocity on membrane surface and aeration amount for controlling membrane fouling were provided.

1. Introduction

In recent years, membrane bioreactor (MBR) system has attracted considerable attentions, especially in advanced wastewater treatment [1–3]. However, the application of MBR is hindered by the problem of membrane fouling which brings the decrease of permeation flux [4–6], as a result, the operation costs of MBR processes are increased with the necessity of cleaning and replacing fouled membranes. Thus, various techniques were introduced to reduce membrane fouling in MBR process [7–9].

Moreover, it is known that the fouling cake forming on the membrane surface not only causes flux reduce and resistance increase, but also enables the separation membranes to reject smaller objects, such as virus, inorganic ions and so on [10]. Thus, a new kind of membrane, made up of common silk and fouling cake, has been developed to actively utilize the separation ability of fouling cake. Based on the fact that the silk with large pores of 50–500 μm has no separation ability, while sludge in reactor is actually rejected by the fouling cake which looks like a new separation membrane added onto the silk, this kind of membrane is thus called dynamic membrane or second membrane [11]. Dynamic membrane not only has almost all characteristics belonging to common membranes, but also has some distinct features, such as low expenditure, low energy consumption and high flux and so on. The dynamic membrane bioreactor (DMBR) is a kind of submerge membrane bioreactor in which the separation membrane is substituted by dynamic membrane.

According to the increasing characteristics of membrane resistance in MBR, the formation process of filtration cake on micro-membrane surface could be divided into blocking stage, transition stage, and cake filtration stage [12]. However, due to the variability of dynamic membrane, the formation mechanism and structure of dynamic membrane in DMBR still have not been completely understood [13]. By far, there are few theories or models about dynamic membrane formation process. So the characteristic and structure of dynamic membrane in DMBR were investigated. The objective of this research was to construct a theory regarding the formation process of dynamic membrane, and develop models for calculating the optimal cross-flow velocity on dynamic membrane surface and optimal aeration amount for membrane cleaning.

2. Blocking filtration laws

The formation of dynamic membrane is a complex process including many physicochemical and microbiological mechanisms, such as internal deposition, pore blocking and cake formation [14]. But in each formation stage, the separation characteristics and structure of dynamic membrane could be well expressed by one main mechanism. Thus, four classic filtration laws (Table 1) originally developed by Hermia for dead-end filtration [15,16], were used to explain the flux behaviors under constant filtration pres-

* Corresponding authors.
E-mail addresses: yangchzh168@126.com (C. Yang), whpu@vip.sina.com (W. Pu).

1385-8947/$ – see front matter © 2008 Elsevier B.V. All rights reserved.
doi:10.1016/j.cej.2008.08.043

Table 1
Empirical dead-end filtration equations.

Law	Description	Equation
Cake filtration	Deposit of particles larger than the membrane pore size onto the membrane surface	$t/V = aV + b$
Complete blocking	Occlusion of pores by particles with no particle superimposition	$-\ln(J/J_0) = at + b$
Intermediate blocking	Occlusion of pores by particles with particle superimposition	$1/J = at + b$
Standard blocking	Deposit of parities smaller than the membrane pore size onto the pore walls, reducing the pore size	$t/V = at + b$

where V is the cumulative volume of permeate at time t; J is the flux; J_0 is the initial flux; and a and b are the model parameters. The linear coefficients, a and b, of the cake filtration model can be related to physical quantities by Eqs. (1) and (2):

$$a = \frac{\mu c_b \alpha_c}{2A^2\,\mathrm{TMP}} \tag{1}$$

$$b = \frac{\mu R_m}{\mathrm{TMP}\,A} \tag{2}$$

where μ is the permeate viscosity, α_c is the specific cake resistance, R_m is the hydraulic resistance of the membrane, TMP is the trans-membrane pressure, A is the membrane surface area, C_b is the concentration of sludge and A is the slope of the best fit of the linear equation: $t/V = f(V)$. Furthermore, the membrane characteristics of voidage, compressibility and height in each phase of the dynamic membrane formation process could be computed out by Eq. (3) and Kozeny Model described as Eqs. (4) and (5):

$$\alpha_c = \alpha_{c_0}\,\mathrm{TMP}^n \tag{3}$$

$$\alpha_c = \frac{180(1-\varepsilon)}{\rho_1 d_p^2 \varepsilon^3} \tag{4}$$

$$\delta_c = \frac{R_c \varepsilon^3 d_p^2}{45(1-\varepsilon)^2} \tag{5}$$

where α_{c_0} is a constant, n is the compressibility factor, the higher the n, the more compressible the cake is. ε is the voidage of the cake, δ_c is the height of the cake, ρ_1 is the density of the wet cake, d_p is the diameter of particles, R_c is the cake resistance.

sure. All models imply a dependence of flux decline on the ratio of the particle size to pore diameter [15].

3. Methods and materials

3.1. Experimental system and analysis

The experimental system used in this test is showed in Fig. 1. The DMBR system consists of a fully mixed biological reactor, a plate–frame membrane module, aeration system and feed pump.

The biologic reactor with a working volume of 7.5 L was manufactured from polyethylene and divided into three parts, namely left, right and middle parts, by barrier plates in the reactor. On the bottom of the left and right parts, several aerators called lateral aeration were set for aeration. On the bottom of the middle part, several aerators called underside aeration were also set. When reactor worked normally, the lateral aeration was operated to provide dissolved oxygen for microorganism, mix the sludge and water, produce cross-flow on the membrane surface and accelerate the circular flow. While the dynamic membrane was fouled so seriously that the reactor was not workable, the lateral aeration was then stopped whereas the underside aeration was operated to remove membrane fouling by strong gas–water multiphase flow.

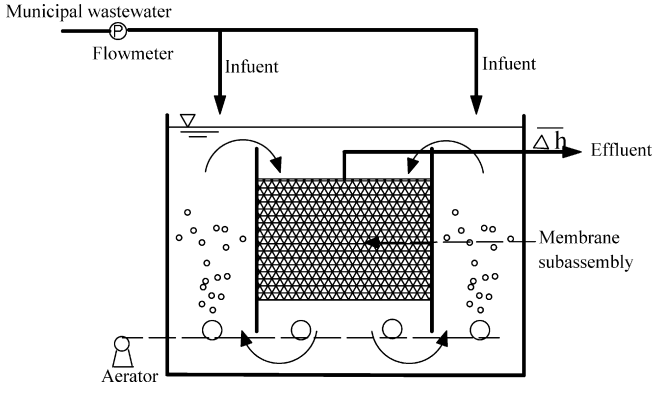

Fig. 1. Diagram of DMBR system.

Table 2
Quality of feed wastewater.

Analysis items	Values
COD (mg/L)	78–126
NH_4^+–N (mg/L)	9–19
TP (mg/L)	1–3
Turbidity (NTU)	56–84
Temperature (°C)	15–24
pH	6–8

Membrane subassembly used in this study is similar to plate–frame membrane. The height and surface area of membrane, made of silk with apertures of 0.1 mm, were 0.1 m and 0.01 m^2, respectively. The permeated water passed through the membrane surface and then effused from reactor. Different from conventional MBRs, the DMBR could be continuously operated for several months until the membrane resistance reached the limited level.

3.2. Methods

The analysis items including pH, DO, COD, NH_4^+–N, turbidity and MLSS were carried out according to the standard methods issued by the China National Environmental Protection Agency [17]. The degree of membrane fouling was calculated using the following resistance model:

$$R = \frac{\mathrm{TMP}}{J\mu} \tag{6}$$

where J is the permeation flux (m^3/m^2 s), μ is the kinetic viscosity of the activated sludge in reactor (Pa s).

3.3. Source of wastewater

This test was feed with the municipal raw sewage, which was screened through 1.0 mm punch holes. The quality of influent is showed in Table 2.

4. Results and discussions

4.1. Hypothetical mechanism for dynamic membrane formation

As a kind of filtration cake, the formation process of dynamic membrane should be similar to that of the fouling cake on micro-membrane and could also be divided into several stages. When MLSS was 7450 mg/L, membrane flux was about 20 L/m^2 h in the first 2 min and was then shortened to 4–10 L/m^2 h for prolonging the durations of each stage. The increasing process of dynamic membrane resistance with operation time is showed in Fig. 2. Results indicate that the formation process of dynamic membrane could be divided into four stages.

4.1.1. Stage 1: substrate formation

Membrane resistance decline occurred in this stage. Due to the large apertures of silk, small sludge particles, colloids and solutes could pass through silk and flow out in the effluent, while large

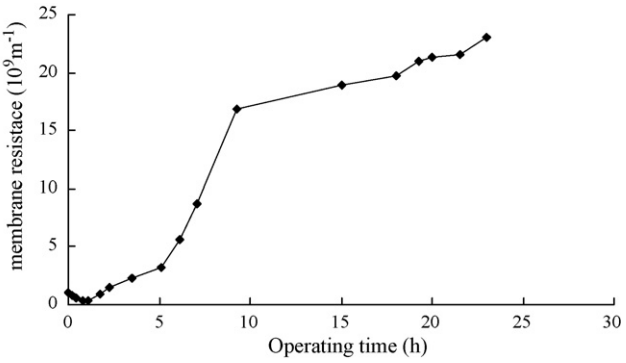

Fig. 2. Variation of membrane resistance with operation time.

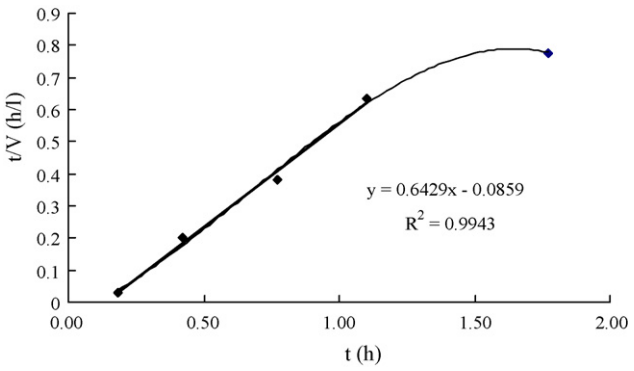

Fig. 3. Linear fitting of the obtained data in phase 1 with standard blocking law.

sludge floc attaching to silk surface could be removed by cross-flow. That is, only the sludge with the size similar to silk aperture could be retained through filling into silk holes. Consequently, the hydrophobic silk is changed to be hydrophilic by the deposition of hydrophilic sludge [18,19], leading to the decline of membrane resistance. According to the analysis, the mechanism underlying substrate formation in this stage should belong to standard blocking model.

4.1.2. Stage 2: separation layer formation

Membrane resistance began to increase, and the increasing rate of resistance became quicker and quicker. In this stage, sludge constituents are accumulated not only on the silk surface, but also on previous deposition layer. Because the formed layers are thinner than the hydrodynamic boundary layer of cross-flow therefore the influence of cross-flow on sludge layer is not obvious, a sludge monolayer called separation layer is thus able to form by removing the sludge with multilayer structure. At the initial period of this stage, a large number of solutes, colloids and small sludge particles could pass through separation layer, indicated by broken sludge bits and high COD content in effluent. However, by accumulating more and more sludge constituents, the aperture of separation layer becomes smaller and smaller, resulting in the ability of dynamic membrane in retaining particles, colloids, virus and even some solutes at last [10]. Thus, in this stage, the mechanism of separation layer formation should be abided with complete blocking model.

4.1.3. Stage 3: fouling layer formation

Increasing rate of membrane resistance became very quick and membrane resistance reached the maximum at the end of this stage. Because the aperture of the dynamic membrane formed in previous stages becomes small enough to retain all sludge components, the sludge layer in this stage could be formed by accumulating solutes, colloids and sludge. Especially, when the influence of the cross-flow on the dynamic membrane becomes intense at the end of this stage, most of large deposited sludge particles are removed, companying with the increase of the solutes and colloids content in dynamic membrane. All those resulted in high membrane resistance. Finally, the resistance of dynamic membrane increases to a steady state at the end of this stage whereas the flux decline rate is further depressed.

4.1.4. Stage 4: filtration cake formation

Membrane fouling rate decreased and reached the steady state. Since the height of dynamic membrane in this stage is already higher than that of hydrodynamic boundary layer, cross-flow plays important roles in further formation process of dynamic membrane and particles deposition are then greatly reduced. In this stage, another important factor influencing membrane resistance is the layer compaction which could increase filtration resistance and decrease permeability. Although sludge layers have been compacted by TMP throughout whole process, its effect becomes far more relevant in stage 4, because a large amount of particles are now being pressurized for a long time. When the permeation drag of the suspended solids is decreased to the back transport velocity, the flux reaches the steady state.

4.2. Testifying hypothetical mechanism

As discussed above, according to the increasing characteristics of membrane resistance with operation time, the formation process of dynamic membrane could be divided into several stages. Moreover, it was found that the resistance of dynamic membrane formed in each stage was much smaller than that formed in the next stage, for several magnitude orders. Therefore, as calculating the resistance of sludge layer formed in each stage, the influence of former layers could not be taken into account. Hence, it is feasible to estimate the filtration model of dynamic membrane in each stage through fitting the experimental data with the four classic filtration laws. When the MLSS is about 7000 mg/L and kinetic viscosity is about 1.17×10^{-3} Pa s, the linear fittings of experimental data in each stage with classic filtration laws are illustrated in Figs. 3–6.

As shown in Fig. 3, the filtration mode in the initial 1 h is well fitted to the standard blocking law, which indicates that substrate formation process is the deposition of particles smaller than the membrane pore into silk holes.

As shown in Figs. 3 and 4, during the period of 1.0–2.0 h, the standard blocking law abided by dynamic membrane filtration is gradually substituted by the complete blocking law. The filtration model of dynamic membrane is perfectly according with the complete blocking law in the period of 1.8–3.5 h, which indicates that separation layer is formed in this stage by monolayer deposition of

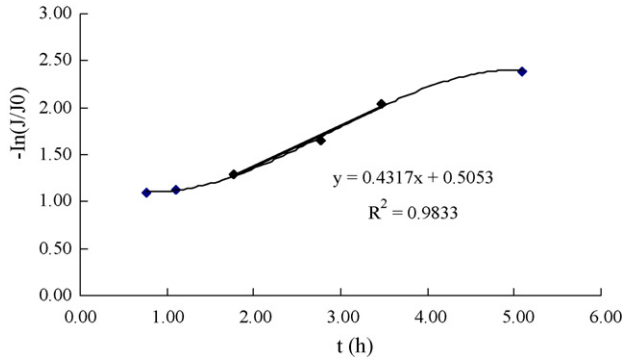

Fig. 4. Linear fitting of the obtained data in phase 2 with complete blocking law.

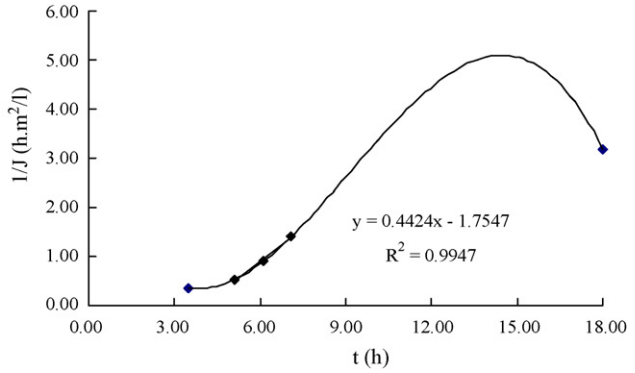

Fig. 5. Linear fitting of the obtained data in phase 3 with intermediate blocking law.

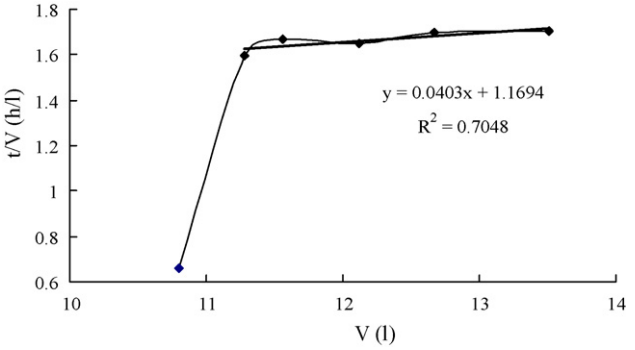

Fig. 6. Linear fitting of the obtained data in phase 4 with cake filtration law.

sludge particles. Furthermore, by analyzing the pollutants content in effluent (Table 5), it is found that the holes of the meshy silk have already been blocked to be small enough to reject almost all sludge components. That is, the separation ability of dynamic membrane in this stage has been comparable to that of micro-membrane and ultra-membrane, and the sludge layers formed in following stages should belong to membrane fouling with little contributions to the improvement of membrane separation ability.

Though dynamic membrane has been reliable to separate effluent after particles depositing into silk holes and pores occluded on silk surface, sludge particles keep on depositing on dynamic membrane surface. In the period of 5.0–7.0 h, the filtration mode of dynamic membrane is well fitted to the intermediate blocking law (Fig. 4). Moreover, it is found that the resistance of dynamic membrane increases most quickly in this stage, implying that it is important to restrain the sludge layer deposited by intermediate blocking law.

At last, the experimental data were tried to fit with cake filtration law (Fig. 5). It is found that throughout the duration of runs, just the filtration mode of dynamic membrane during the period of 11.0–14.0 h could be described by the cake filtration law, which indicated that filtration cake is formed in this stage by depositing of particles larger than the membrane pore.

4.3. Characteristics of dynamic membrane formed in each stage

4.3.1. Cake compressibility

The α_c values of filtration layers formed in stages 1–4, calculated according to the standard blocking law, complete blocking law, intermediate law and cake filtration law, are 1.25×10^{15}, 1.95×10^{15}, 7.22×10^{15} and 3.53×10^{15} m/kg, respectively. Based on the established formation mechanisms, the sludge layer in stage 1 is formed by particles deposition into silk holes and thus could be considered as incompressible. That is, n and α_c values in stage 1 could be considered as zero and α_{c_0}, respectively. Then, the n values of stages 2–4 are calculated out as 0.0158, 0.0597 and 0.0374, respectively. It is obvious that the relatively low compressibility of cake is formed in stage 2, while higher compressibility is obtained for stage 3 than stage 4.

Different cake compressibility of the sludge layers formed in each stage might be induced by the shifts of formation mechanisms. As mentioned above, the sludge layer formed in stage 2 is a particles monolayer with few compressible voids in the vertical direction of dynamic membrane surface, resulting in low compressibility. In stage 3, the sludge layer is formed by one particle depositing onto another, producing huge compressible void and inducing the largest n value. Basically, the sludge layer formed in stage 4 should have the highest compressibility. However, because the height of dynamic membrane in stage 4 is already larger than that of hydrodynamic boundary layer, the loose components in dynamic membrane could be removed by cross-flow while the compact structure is accumulated, resulting compressibility reduce in stage 4.

4.3.2. Voidage and height of filtration cake

The voidage value (ε) of filtration cake formed in stage 4 is calculated by Eq. (4) as about 0.162, larger than that of alginate cake on micro-membrane surface, from 0.078 to 0.078 [16]. Moreover, the height of filtration cake is also calculated by Eq. (5) as about 41.07 mm, which is much larger than the value of 10–20 mm measured by the ruler installed vertically against membrane surface. This difference might be contributed by the influence of cross-flow on membrane surface.

4.4. Structure of dynamic membrane

Based on the results analyzed above, dynamic membrane from inner to outer could be divided into three layers (Fig. 7):

- Substrate layer made up of silk and large particles with diameter of about 0.1 mm.
- Separation layer made of sludge particles whose size is decreased from inner to outer, and the separation ability of this layer is comparable to micro-membrane.
- Fouling layer made up of sludge particles, solutes and colloids.

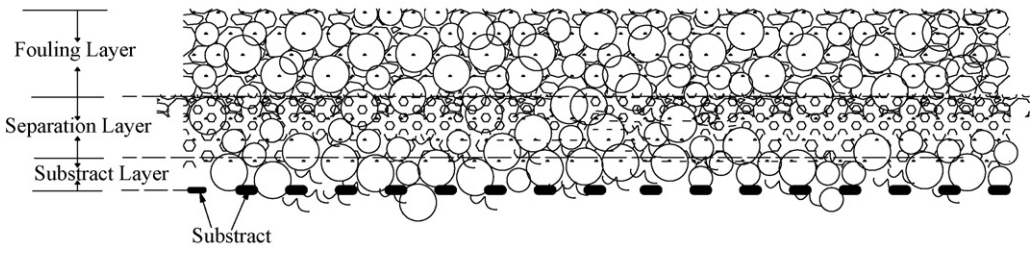

Fig. 7. Diagram of dynamic membrane structure.

4.5. Application of dynamic membrane formation mechanisms

4.5.1. Optimum cross-flow rate

Based on the theory of hydrokinetic boundary layer, it is known that there is a hydrodynamic boundary layer on the membrane surface when liquid flows along the membrane surface, and the influence of cross-flow on the dynamic membrane surface is very limited when the height of dynamic membrane is less than that of hydrodynamic boundary layer. Moreover, the height of hydrodynamic boundary layer could be controlled by adjusting cross-flow rate when other parameters, such as viscosity of the mixture, temperature and so on, are kept immobile. Thus, the height of hydrodynamic boundary layer could be adjusted to an optimum spectrum, which includes the filtration layers to ensure the separation ability of dynamic membrane but excludes the fouling layer to reduce the membrane resistance. Furthermore, based on the established mechanism, the optimum height of hydrodynamic boundary layer should be equal to the height of the separation layer and could be obtained by adjusting cross-flow velocity.

When the cross-flow is provided by the lateral aeration, mixed liquor in reactor is Newton liquid and flow pattern of cross-flow is laminar flow. The optimal cross-flow rate on the dynamic membrane surface could be obtained by the following method deduced by the theory mentioned above.

4.5.1.1. Calculating the height of hydrodynamic boundary layer. The height of hydrodynamic boundary layer could be calculated by the model of the plate-laminar-flow hydrodynamic boundary:

$$\delta = 5.477\sqrt{\frac{\upsilon x}{U_0}} \tag{7}$$

where δ is the height of the hydrodynamic boundary layer, υ is the permeate kinematic viscosity, U_0 is the rate of the flow in front of the membrane, x is the smallest distance in the direction of the cross-flow between the point with flow rate of U_0 and the front top of the membrane.

4.5.1.2. Calculating the height of dynamic membrane. By combining Eqs. (4) and (5), the height of dynamic membrane (δ) could be described as below:

$$\delta = \frac{4\mathrm{TMP}}{\alpha_c J \mu \rho_2 (1-\varepsilon)} \tag{8}$$

where α_c is the specific cake resistance, ε is the voidage of the dynamic membrane and ρ_2 is the density of the mixture in the reactor.

4.5.1.3. Optimum cross-flow rate. According to the theoretical analysis above, the optimum cross-flow rate could be calculated by the following equation:

$$U_0 = \frac{1.9\upsilon x \alpha_c^2 J^2 \mu^2 \rho_2^2 (1-\varepsilon)^2}{\mathrm{TMP}^2} \tag{9}$$

4.5.2. Optimum aeration gas amount for controlling membrane fouling

When dynamic membrane is fouled so seriously that the reactor is not workable, the gas–liquor multiphase flow provided by underside aeration is necessary to remove membrane fouling. The optimum aeration amount could be calculated by following method.

4.5.2.1. Calculating Reynolds number of turbulent flow. The cross-flow provided by underside aeration is not laminar flow now, but turbulent flow. The characteristics of the turbulent flow could be described by Reynolds number and skin friction coefficient, both of which could be calculated out by the model of calculating the height of turbulent flow boundary layer (Eq. (10)) and Prandtl–Karman model (Eq. (11)):

$$\frac{\delta_b}{D} = \frac{5\sqrt{2}}{Re\sqrt{f}} \tag{10}$$

$$\frac{1}{\sqrt{f}} = 4.0\lg(Re\sqrt{f}) - 0.4 \tag{11}$$

where δ_b is the height of the flow boundary layer, D is the equivalent diameter ($D = 4r$, r is hydraulic radius), Re is the Reynolds number according with equivalent diameter and f is skin friction coefficient.

Table 3
The maximal velocity of the air bubble in the water with one kind of gas.

Scope	The maximal velocity of air bubble	The range of Reynolds number
Zone 1	$\upsilon_\infty = \frac{2R_b^2(\rho_f-\rho_g)g}{9\mu f}$	$Re < 2$
Zone 2	$\upsilon_\infty = 0.33g^{0.76}\left(\frac{\rho_f}{\mu_f}\right)^{0.52}R_b^{1.28}$	$2 < Re < 4.02G_1^{-2.214}$
Zone 3	$\upsilon_\infty = 1.35(\sigma/\rho_f R_b)^{0.50}$	$4.02G_1^{-2.214} < Re < 3.10G_1^{-0.25}$ or $16.32G_1^{0.144} < Re < 5.75$
Zone 4	$\upsilon_\infty = 1.18(g\sigma/\rho_f)^{0.25}$ (1.18 is usually substituted by 1.53)	$3.10G_1^{-0.25} < Re$ $5.75 < G_2$

where Re is the Reynolds number, υ_∞ is the maximal velocity of air bubble and Re_b, G_1, G_2 could be calculated by Eqs. (12)–(14):

$$Re_b = \frac{2\rho_f \upsilon_\infty R_b}{\mu_f} \tag{12}$$

$$G_1 = \frac{g\mu_f^4}{\rho_f \sigma^3} \tag{13}$$

$$G_2 = \frac{gR_b^4 \upsilon_\infty^4 \rho_f^3}{\sigma^3} \tag{14}$$

4.5.2.2. Calculating the velocity of air bubble on membrane surface. The maximal velocity of air bubble on the surface of membrane in aeration process could be calculated by the models listed in Table 3.

4.5.2.3. Calculating the flow velocity on membrane surface. It is known that in the gas–liquor multiphase flow, the velocity of the liquor flow is slower than that of the gas flow. There is a relationship between the liquor flow velocity (υ_L) and gas flow velocity (υ_g), and the value of υ_g/υ_L could be calculated out by the following equation:

$$s = 1 + \frac{\rho' a}{(1-M)G} \tag{15}$$

where s is the value of υ_g/υ_L, ρ' is the density of the liquor, a is the coefficient involving pressure and conduit diameter, G is the mass flux and M is the weight of the dry activated sludge with unit volume.

Table 4
Performance of DMBR with MLSS of about 3000 mg/L.

Indexes	COD (mg/L)	Turbidity (NTU)	NH_4^+–N (mg/L)	TP (mg/L)
Influent	134.6	89.6	28.0	1.9
Effluent	28.2	3.2	2.1	0.5
Removal rate (%)	77.9	96.3	91.7	72.6

Table 5
Performance of DMBR with MLSS of about 7450 mg/L in an operation cycle.

	Time (min)								
	5	15	30	60	120	240	480	720	1500
Effluent COD (mg/L)	135.8	80.6	75.6	50	46.8	–	30.3	–	32.5
Effluent turbidity (NTU)	78	60	56	20	16	5	2.5	2.1	2.0

4.5.2.4. Calculating the optimum aeration amount. By deducing Eq. (12), R_b could be calculated from the following equation:

$$R_b = \frac{Re_b \mu_f}{2\rho_f \upsilon_\infty} \tag{16}$$

When the liquor is viscous, the volume of a single gas bubble could be calculated by Davison-Schuler model:

$$V_b = \left(\frac{4}{3}\pi\right)^{1/4} \left[\frac{15\mu Q_g}{2g(\rho_3 - \rho_g)}\right]^{3/4} \tag{17}$$

Based on the established mechanisms, the model for calculating the optimum aeration amount could be built up as follows:

$$Q_g = \frac{2g(\rho_3 - \rho_g)}{15\mu} \left[\frac{4}{3}\pi R_b^3 \left(\frac{4}{3}\pi\right)^{1/4}\right]^{3/4} \tag{18}$$

where V_b is the volume of the air bubble, ρ_3 and ρ_g are the density of the liquor and gas, respectively, Q_g is the aeration gas amount and R_b is the equivalent radius of the air bubble.

4.6. Performance of DMBR system

In this study, the test could be divided into two stages, namely low MLSS and high MLSS. At low MLSS of about 3000 mg/L, dynamic membrane have been continuously operated for several months without membrane cleaning and perfect separation ability of dynamic membrane could be obtained within 30 min, which has been reported in our previous work [20]. Moreover, when MLSS is about 3000 mg/L, DO is 2.0–3.0 mg/L and pH is 6.0–7.0, the average performance of DMBR within 1 month is showed in Table 4.

In order to describe the formation process of dynamic membrane more visually, the MLSS was improved for shortening the operation cycle of dynamic membrane. When MLSS is about 7540 mg/L, COD and turbidity in influent are 215.5 mg/L and 150.0 NTU, respectively, DO is 2.0–3.0 mg/L and pH is 6.0–7.0, the performance of a typical operation cycle of about 25 h is showed in Table 5. It is found that COD and turbidity contents in the effluent reach stable after 5 h, implying that the complete formation of dynamic membrane at high MLSS of 7540 mg/L required 5 h, much longer than that of low MLSS. Therefore, in the system of DMBR, it is very important to control MLSS within an effective range.

4.7. Conclusion

Dynamic membrane is formed during the filtration process and varies with the operation time. Thus, it is difficult to express the formation mechanisms of dynamic membrane by mathematical model. Based on the flux behaviors under constant filtration pressure, the formation mechanisms of dynamic membrane was developed by dividing formation process into four stages, which was then testified by the four classic filtration laws. Moreover, dynamic membrane from inner to outer was divided into three layers, namely substrate layer, separation layer and fouling layer. Then, by combining the established mechanisms with the theory of hydrokinetic boundary layer, the method for calculating the optimal cross-flow rate on the dynamic membrane surface was developed, and the model for calculating the optimal aeration amount to control membrane fouling was built up.

Acknowledgement

This research was supported by Natural Project of China for the development of advanced technologies (No. 2003AA601110).

References

[1] M. Vocksa, C. Adama, B. Lesjean, Enhanced post-denitrification without addition of an external carbon source in membrane bioreactors, Water Res. 39 (2005) 3360–3368.
[2] M. Brik, P. Schoeberl, B. Chamam, Advanced treatment of textile wastewater towards reuse using a membrane bioreactor, Process Biochem. 41 (2006) 1751–1757.
[3] F. Fatonea, D. Bolzonellaa, P. Battistoni, Removal of nutrients and micro pollutants treating low loaded wastewaters in a membrane bioreactor operating the automatic alternate-cycles process, Desalination 183 (2005) 395–405.
[4] R. Liu, X. Huang, C.W. Wang, Membrane fouling control in an integrated membrane bioreactor, Environ. Sci. (China) 21 (2000) 58–61.
[5] E.H. Bouhabila, R.B. Aim, H. Buisson, Fouling characterization in membrane bioreactors, Sep. Purif. Technol. 2223 (2001) 123–132.
[6] L. Defrance, M.Y. Jaffrin, B. Gupta, Contribution of various constituents of activated sludge to membrane bioreactor fouling, Bioresource Technol. 73 (2000) 105–112.
[7] H.C. Chua, T.C. Arnot, J.A. Howell, Controlling fouling in membrane bioreactors operated with a variable throughput, Desalination 149 (2002) 225–229.
[8] A. Sofia, W.J. Ng, S.L. Ong, Engineering design approaches for minimum fouling in submerged MBR, Desalination 160 (2004) 67–74.
[9] S.P. Hong, T.H. Bae, T.M. Tak, Fouling control in activated sludge submerged hollow fiber membrane bioreactors, Desalination 143 (2002) 219–228.
[10] C. Chiemchaisri, Y.K. Wong, T. Urase, Organic stabilization and nitrogen removal in membrane separation bioreactor for domestic wastewater treatment, Filtr. Sep. 30 (1993) 247–252.
[11] J. Lee, W.Y. Ahn, C.H. Lee, Comparison of the filtration characteristics between attached and suspended growth microorganisms in submerged membrane bioreactor, Water Res. 35 (2001) 2435–2445.
[12] J. Tao, D. Maria, Kennedy, The role of blocking and cake filtration in MBR fouling, Desalination 157 (2003) 335–343.
[13] C.Z. Yang, H.B. Liu, W.H. Pu, et al., Self-forming dynamic membrane bio-reactor for domestic wastewater treatment, China Water and Wastewater 22 (2006) 105–108.
[14] T.H. Bae, T.M. Tak, Interpretation of fouling characteristics of ultrafiltration membranes during the filtration of membrane bioreactor mixed liquor, J. Membr. Biol. 264 (2005) 151–160.
[15] Y. Ye, E. Le Clech, V. Chen, Fouling mechanisms of alginate solutions as model extra cellular polymeric substances, Desalination 175 (2005) 7–20.
[16] J. Hermia, Constant pressure blocking filtration laws-application to power-law non-Newtonian fluids, Trans. IchemE 60 (1982) 183–187.
[17] S.E.P.A. Chinese, Water and Wastewater Monitoring Methods, Chinese Environmental Science Publishing House, Beijing, 1997.
[18] Y. Zhou, Research on Low C/N and High Ammonia Nitrogen Content Sewage by Self-forming Bio-dynamic Membrane Reactor, Paper for Master Thesis, Huazhong University of Science and Technology, China, 2006, pp. 20–21.
[19] J.Y. Wu, Research on the Self-forming Bio-dynamic Membrane Reactor for Urban Wastewater Treatment, Master Thesis, Normal school of Shanghai, Shanghai, China, 2004.
[20] H.B. Liu, C.Z. Yang, W.H. Pu, et al., Application of the self-forming bio-dynamic membrane reactor in treatment of municipal sewage, Technol. Treat. Water (China) 11 (2007) 67–70.